JOURNAL OF PROPULSION AND POWER
Vol. 21, No. 3, May–June 2005

Mass Spectrometric Analysis of Colloid Thruster Ion Emission from Selected Propellants

Yu-Hui Chiu,* Brad L. Austin,† and Rainer A. Dressler*
U.S. Air Force Research Laboratory, Hanscom Air Force Base, Massachusetts 01731
Dale Levandier‡
Boston College, Newton, Massachusetts 02159
P. Terrence Murray§
University of Dayton, Dayton, Ohio 45469
and
Paulo Lozano¶ and Manuel Martinez-Sánchez**
Massachusetts Institute of Technology, Cambridge, Massachusetts 02139

Retarding potential, time-of-flight (TOF), and quadrupole mass spectrometric methods are applied to study the charged species emitted from a colloid thruster operated in a cone-jet mode at high-specific-impulse operating conditions. Measurements are conducted for two propellants, a 28.4 wt% NaI/formamide electrolyte solution and the ionic liquid 1-ethyl-3-methylimidazolium tetrafluoroborate ([EMIM][BF_4]). When operated at a volume flow rate of 2–6 $\times 10^{-14}$ m^3/s and a positive polarity, the electrolyte solution yields an average specific charge, q/m, of $\sim$11,000 C/kg with an ion/droplet current ratio of 9 to 1. Fully angularly integrated TOF measurements determine an average mass-to-charge ratio of 253 atomic mass units. The axial quadrupole mass spectrometric measurement identifies solvated sodium ions, $Na^+(HCONH_2)_n$ ($n = 1, \ldots, 10$), with a distribution peaked at $n = 4$. Stopping potential and retarding potential measurements suggest that most charged particles are produced with energies $\sim$200 V below the capillary bias potential. The inability to operate this propellant in a pure ion emission mode makes the thruster inefficient when operated in the ion-evaporation, high-specific-impulse conditions. The ionic liquid, [EMIM][BF_4], is operated in a pure ion emission mode for both positive and negative polarity, yielding mean specific charges exceeding 250,000 C/kg. X([EMIM][BF_4])$_n$ ($n = 0, 1, 2$) ions, where X = $EMIM^+$ or BF_4^-, are identified. Contrary to the electrolyte solution, the energy analysis of the field-evaporated ions reveals that the ions are produced at the capillary potential with a narrower energy width of 50 V. For an acceleration voltage of 1500 V, a specific impulse of $\sim$4000 s at an efficiency exceeding 90% is recorded.

Nomenclature

E	=	ion energy at detector
E_{th}	=	molecular thermal energy exceeding zero-point energy
E_0	=	parent ion energy
g	=	Earth's acceleration
I	=	total output current
I_{cor}	=	corrected mass spectral intensity with respect to ion decay patterns
I_{raw}	=	observed mass spectral intensity
I_{sp}	=	specific impulse
l	=	number of lost solvent molecules
m	=	particle mass
$\dot{m}$	=	mass flow rate
m/q	=	mass-to-charge ratio
m_s	=	solvent molecule mass
m_0	=	parent ion mass
n	=	solvation number
Q	=	volume flow rate
q	=	particle charge
q/m	=	specific charge
T	=	thrust
V_a	=	extraction voltage
V_c	=	capillary potential
V_e	=	extractor potential
η	=	thrust efficiency

Presented as Paper 2003-4848 at the AIAA/ASME/SAE/ASEE 39th Joint Propulsion Conference, Huntsville, AL, 20–23 July 2003; received 13 April 2004; revision received 9 June 2004; accepted for publication 23 August 2004.

*Task Scientist, Space Vehicles Directorate. Member AIAA.
†Second Lieutenant, Space Vehicles Directorate.
‡Staff Scientist, Institute for Scientific Research.
§Professor, Graduate Materials Engineering.
¶Postdoctoral Research Associated, Space Propulsion Laboratory. Member AIAA.
**Professor of Aeronautics and Astronautics, Space Propulsion Laboratory. Member AIAA.

Introduction

COLLOID thrusters and field emission thrusters (FEEPs) are based on the extraction and acceleration of charged species from conducting liquids using high electric fields.[1–3] They represent one of the most attractive forms of microelectric propulsion due to their high efficiency because they do not depend on a discharge to create the charged particles. Contrary to FEEPs that employ liquid metal propellants that emit atomic metal ions, the main fraction of the charged-particle current observed from colloid thrusters has been saturation-charged droplets with a minor fraction attributable to molecular ions. Consequently, colloid thrusters operate at higher thrusts and lower specific impulses than FEEPs.

It has recently been discovered that colloid thrusters operated in a novel cone-jet mode (single Taylor cone) with a high-conductivity electrolyte solution, NaI in formamide, at a very low liquid volume flow rate and low extraction voltages can produce much higher fractions of molecular ions.[4–6] The enhanced ion emission is attributed to field evaporation of ions that occurs when the electric field strength at the liquid surface increases above 1 V/nm. The high electric fields stem from high cone curvatures arising when the volume flow rate is reduced.[4,7] This new mode of operation for

colloid thrusters is highly attractive because it results in a significant increase of the thruster specific impulse and thus extends the specific impulse range of a colloid thruster, thereby enabling greater mission planning flexibility. Furthermore, the thruster can be operated at lower voltages more amenable to miniaturization. The exploitation of this field-evaporation mode calls for an improved understanding of this new domain of electrospray physics that involves ion extraction from a liquid jet subjected to nanometer dimensions. A first step in this direction is to identify and characterize the charged species emitted from the liquid; m/q and the energy distributions of the ions are measures of thrust, specific impulse, and efficiency of the colloid thruster. Gamero-Castaño et al.[4–6] and Lozano and Martinez-Sánchez[8,9] conducted time-of-flight (TOF) and stopping potential (SP) measurements of the NaI/formamide propellant to estimate the specific charge and measure the energy of field evaporated ions, respectively. Precise identification and distributions of the ions could not be made due to the lack of TOF resolution.

In the present work, we complement the TOF and SP approach with higher resolution mass spectrometric measurements to precisely identify the mass-to-charge ratio, m/q, of the ions produced in the low-flow-rate cone-jet mode of operation. The present work presents the first application of a quadropole mass filter for the analysis of colloid thruster emissions. Apart from providing new insights into the relationships among propellant, operating conditions, and performance, a primary objective of this work is to evaluate the suitability of mass spectrometers for colloid thruster performance diagnosis. Results are presented for two promising propellants for which high field-evaporation rates have been observed: an electrolyte solution, 28.4 wt% NaI in formamide ($HCONH_2$), and an ionic liquid, 1-ethyl-3-methylimidazolium tetrafluoroborate ([EMIM][BF_4]). Ionic liquids are particularly attractive propellants for colloid thrusters due to their negligible vapor pressures, significant conductivities, and solventless composition. In fact, very recently pure ionic emission from [EMIM][BF_4] has been discovered and reported, thus laying the foundation for a very-high-specific-impulse colloid thruster.[10,11]

Experimental

Colloid Thruster

The thruster capillary is made of fused silica with an inner diameter (i.d.) of 20 μm and tapered down to a 5-μm-tip diameter (New Objective, Inc.). The propellant is transported from a reservoir to the capillary using a 50-μm-i.d. fused silica capillary that is coupled to the thruster capillary using a capillary union (Upchurch Scientific). A constant pressure of nitrogen inside the reservoir regulates the flow rate of the propellant.[9] The combination of a nitrogen valve and a mechanical pump are used to adjust the reservoir pressure, which is monitored using a pressure transducer (MKS instruments). The flow rate is determined from the velocity of a bubble introduced into the capillary. The flow measurement as well as Taylor cone observations are carried out with the visual aid of a video microscope (800 × magnification, Scienscope). All measurements of the present work are carried out at room temperature.

The NaI/formamide 28.4 wt% solution has a conductivity of 2 S/m. The ionic liquid, [EMIM][BF_4], has a conductivity of 1.3 S/m and was used without further purification (Sigma-Aldrich Corp.). The mass spectrometer transmission calibration compound, FC-43 or perfluorotributylamine, was also used without further purification (Scientific Instrument Services).

Time-of-Flight Apparatus (Massachusetts Institute of Technology)

The TOF apparatus, schematically shown in Fig. 1, has been described in detail previously,[8,9] and so only a brief outline is given here. The thruster source is positioned ahead of an extractor ion-optical assembly and an electrostatic gate that has the purpose of pulsing the charged particle flux. Following traversal of a flight tube of variable length L_0, the charged particles are detected either with a collector plate or a channel electron multiplier. In collector plate measurements, collection efficiency is assessed by comparing the measured current to the total current leaving the capillary. A pair of grids located just ahead of the detector is used to retard the

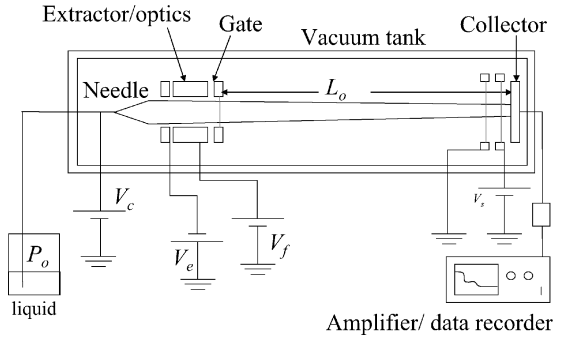

Fig. 1 Schematic diagram of the TOF apparatus at Massachusetts Institute of Technology.

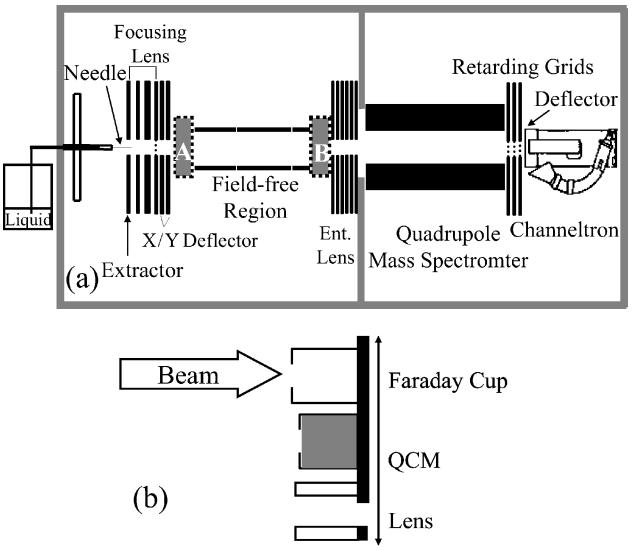

Fig. 2 Schematic diagram of the quadrupole mass spectrometer at AFRL: a) shaded areas A and B represent vertically translatable objects, where A is a near-field target shown in b), and B is a current flag.

particle flux. This permits the recording of simultaneous TOF and SP measurements. The former are obtained from recording the time-resolved emission current either after rapidly deflecting the thruster plume with the electrostatic gate from the axis to prevent charged particles from reaching the detector or by pulsing the extraction gate in a way that the thruster plume is only briefly propagated on-axis. SP measurements are obtained by ramping a voltage on the second of the two grids situated in front of the detector.

Mass Spectrometer (U.S. Air Force Research Laboratory)

The mass spectrometric experiment uses a quadrupole mass filter. Quadrupoles are well suited for this application because their mass settings are not dependent on the ion energy, contrary to TOF measurements and magnetic sector instruments. The mass resolution, however, is reduced as the ion transmission energy increases. A schematic diagram of the quadrupole mass spectrometric apparatus is shown in Fig. 2. The apparatus consists of a source and detector high-vacuum chamber, each evacuated by a 250 l/s turbo pump. The base pressures are $\sim 5 \times 10^{-7}$ and 5×10^{-8} torr, respectively.

The thruster capillary is positioned within 1 mm from the extractor orifice, which has an i.d. of 6 mm. In this geometry, typical extraction voltages used for 28.4 wt% NaI/formamide and [EMIM][BF_4] are 2000 and 2700 V, respectively. The beam of charged particles is then focused and directed onto a near-field target by a set of lenses and a pair of x and y deflectors, shown in Fig. 2b. The near-field target consists of a linear translation manipulator to which three objects are mounted vertically: a Faraday cup assembly with an entrance aperture of 6 mm, a quartz-crystal microbalance (QCM; XTM/2, Inficon) with an equally sized aperture, and a cylindrical lens element for beam transmission. The near-axial thrust current or mass flow

rate is measured by positioning the Faraday cup or the QCM on the thrust axis, respectively. The mass flow rate, determined from the QCM mass deposition measurement, has an estimated uncertainty of ~20%. From a comparison of the total current emitted from the capillary and the mass flow retrieved from the bubble velocity measurement, it is concluded that the near-field measurements comprise between 10 and 50% of the total mass and charged-particle flux, depending on the focusing potentials and the propellant used. For the operation conditions of the present work, the collection efficiency at the near-field probes is ~44% and ~14% for the 28.4 wt% NaI/formamide solution and [EMIM][BF_4], respectively.

When the lens element is positioned on the thrust axis, the accelerated charged species are directed through a field-free region and injected into a quadrupole mass filter (9.5 mm-diameter rod, Extrel ABB) using a set of focusing lenses. The solid angle of collection can be affected by the focusing lens but in all cases is substantially smaller than in the TOF experiments. Thus, the mass spectral measurements must be regarded to reflect on-axis conditions. The mass filter can be operated in either an rf-only all-pass, single-mass selection, or a mass scanning mode. The ions transmitted through the filter are then passed through a set of three grids used for the retarding potential analysis of ion energies, and onto an off-axis channeltron detector (Burle Electro-Optics), which can be operated in either a positive or negative pulse counting mode. Standard electronics are used to process the ion signals. While scanning a mass spectrum, the retarding grids are set to ground potential. The current arrangement allows for ion energy distribution measurements for a particular mass-to-charge ratio, m/q. To obtain a retarding potential energy curve for a specific ion mass, the quadrupole mass filter is set to transmit an m/q value of interest while the voltage applied to the central grid of the retarding grid assembly is scanned. Only a small fraction of the total emitted current is allowed to reach the channeltron detector to prevent saturation of the detector.

Mass calibration and the mass-dependent transmission function and detector response are obtained from an electron-impact ionization study of a standard compound, FC-43, with known fragmentation pattern at an electron energy of 70 eV. An electron impact source was positioned in front of the entrance lens stack of the quadrupole. The intensities of fragmented ions of FC43 were measured for all investigated quadrupole transmission energies, from which the mass-dependent discrimination correction factors were determined. The most significant mass discrimination is observed at high energies and high mass.

Results

NaI/Formamide Solution

Figure 3 is a TOF measurement for the 28.4 wt% NaI/formamide solution operated at a minimum volume flow rate of ~0.05 nl/s or 5×10^{-14} m^3/s. The capillary potential was +1 kV with respect to ground and the flight tube, and the length of the tube was $L_0 = 0.742$ m. The extraction voltage was 1.2 kV, and a total output current of ~600 nA was registered. The time-resolved current exhibits two steps: a larger step at 29 μs and a second, broader step at longer flight times of ~170 μs. Figure 4 is an SP measurement taken in the same instrument at the same conditions, indicating a relatively broad-charged particle energy distribution centered at a potential of 840 V, which is 160 V below the capillary potential. From the measured charged-particle energy, the analysis of the flight times yields a specific charge, q/m, of $(3.82 \pm 0.60) \times 10^5$ C/kg for the large step with a mean flight time of 29.3 μs, corresponding to a mass-to-charge ratio of 253 ± 38 atomic mass units (amu), whereas the second step represents a q/m of ~11,000 C/kg or ~9000 amu. From the mass-to-charge ratios it can be clearly concluded that the fast charged particles are ions whereas the slow charged particles are multiply charged droplets. Unless the ion fraction in the beam is close to unity, most of the mass flow results from the heavier droplets, which therefore govern the thrust and specific impulse.

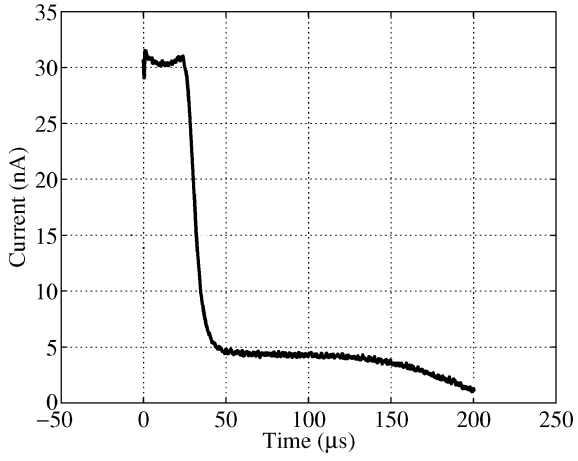

Fig. 3 TOF measurement of the plume from a 28.4 wt% NaI/formamide solution at 1 kV capillary potential with respect to the flight tube ground.

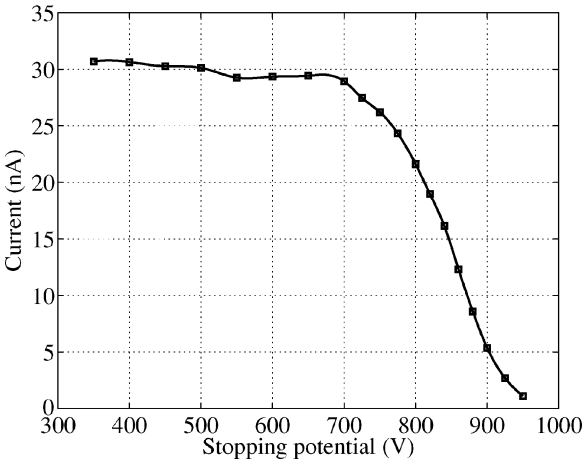

Fig. 4 Stopping potential measurement (TOF apparatus) of the plume from a 28.4 wt% NaI/formamide solution at the same conditions of Fig. 3.

In the near-field measurements of the mass spectrometer, the average charge-to-mass ratio, q/m, is determined from the total current measured on the Faraday cup, I, and the mass deposition rate, $\dot{m}$, measured on the QCM:

$$q/m = I/\dot{m} \tag{1}$$

The q/m value of ~11,000 C/kg, derived from mass deposition rates and currents of 1.05×10^{-7} A and 1.03×10^{-8} g · s^{-1}, respectively, is in good agreement with the TOF results for the droplet component. Mass deposition rates determined with a QCM could result in erroneous readings at high particle energies due to sputtering and droplet splattering or solvent evaporation. We have, therefore, measured the mass deposition rate as a function of capillary potential while maintaining a constant extraction voltage: $V_a = V_c - V_e = 2000$ V. Thus, we determine the apparent specific charge as a function of ion and droplet QCM impact energy, which is given by the capillary potential because the QCM is operated at ground potential. The measured apparent specific charge is plotted as a function of capillary potential in Fig. 5. The apparent q/m value is relatively independent of impact energy at capillary potentials ranging from 350 to 900 V. The apparent q/m value starts to increase sharply with capillary potential at higher potentials and rises with decreasing potential at low potentials. The increase at high capillary voltage (i.e., high impact energies) indicates that ion sputtering and solvent evaporation may be important, resulting in a reduced mass deposition measurement. The reason for the high apparent q/m values at low energies is not clear but is most likely due to divergence problems at these particle energies. Because solvent evaporation from the QCM surface cannot be ruled out, the determined specific charge must be considered an upper limit. The average q/m value obtained at $V_c = 550$ V is, however, in good agreement with the TOF apparatus value. The

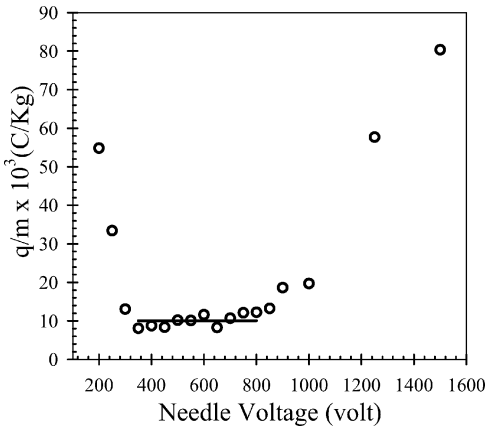

Fig. 5 Apparent q/m as a function of the capillary potential as determined with the near-field probes of the quadrupole apparatus. The solid line indicates an average q/m of $(10.1 \pm 1.6) \times 10^3$ C/kg.

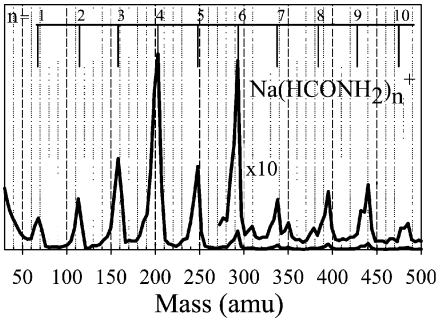

Fig. 6 Typical mass spectrum for a 28.4 wt% NaI/formamide solution, an extraction voltage of 2000 V ($V_c = 550$ V, $V_e = -1450$ V), and 2×10^{-14} m^3/s flow rate. The main peaks are attributed to different solvation numbers n of solvated formamide ions.

agreement between the two methods, whereby the TOF method is fully angularly integrated, suggests that the specific charge does not exhibit a dramatic angular dependence. Furthermore, the q/m measurements are consistent with values determined from the total current, leaving the capillary and the mass flow rate determined with the bubble method, further suggesting that sputtering, and possible droplet splattering, does not significantly affect the current measurement.

Figure 6 shows a typical mass spectrum of the NaI/formamide solution at an extraction voltage of 2000 V and a 2×10^{-14} m^3/s flow rate. The signal below 50 amu is due to ions that are not discriminated by the mass filter due to the low rf amplitude and high transmission energy. At higher mass values, a series of equally spaced peaks is observed that can be attributed to solvated sodium ions: $Na^+(HCONH_2)_n$ $(n = 1, \ldots, 10)$. The $n = 4$ solvated ion is found to be the most abundant species. The spectrum corresponds to an average q/m of 193 amu, which corresponds to an average solvation number of 3.8. This value is slightly lower than the m/q value of 253 $\pm$ 38 amu, corresponding to an average solvation number $n = 5.1$, determined in the TOF measurements for the ion component. The spectrum in Fig. 6 shows no evidence for multiply charged ions.

Figure 7 compares mass spectra observed at different flow rates of $\sim 2 \times 10^{-14}$ m^3/s and $\sim 2 \times 10^{-13}$ m^3/s, respectively. The extraction voltages were 2000 and 2100 V, respectively. The specific charges determined with the near-field probes are $\sim$11,000 and 1500 C/kg for the low and high flow rates, suggesting significantly larger droplets in the high-flow-rate case. The mass spectra exhibit minor differences with a minor shift to lower masses at the higher flow rate. The average m/q for the low- and high-flow-rate cases are 212 and 190 amu, respectively. The change in average atomic mass units from the low-flow-rate measurement of Fig. 6 and that of Fig. 7 reflects the reproducibility of conditions of the present experiment.

Figure 8 compares retarding potential measurements for different mass filter settings. The capillary potential for this measurement was

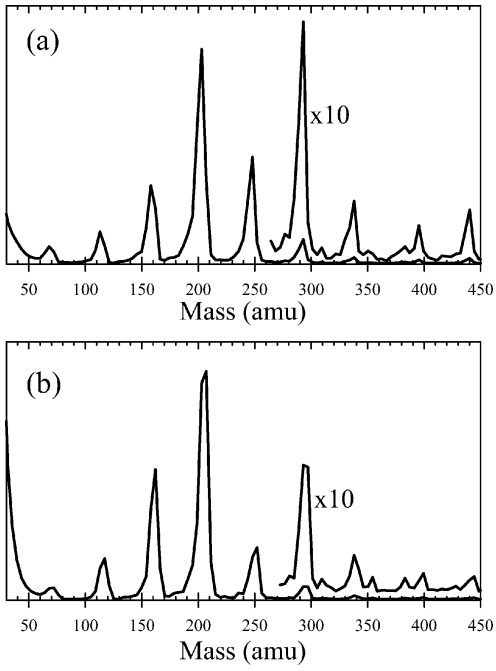

Fig. 7 Mass spectrum of NaI/formamide solution taken at a) a flow rate of 2×10^{-14} m^3/s and acceleration voltage of 2000 V and b) a flow rate of 2×10^{-13} m^3/s and extraction voltage of 2100 V.

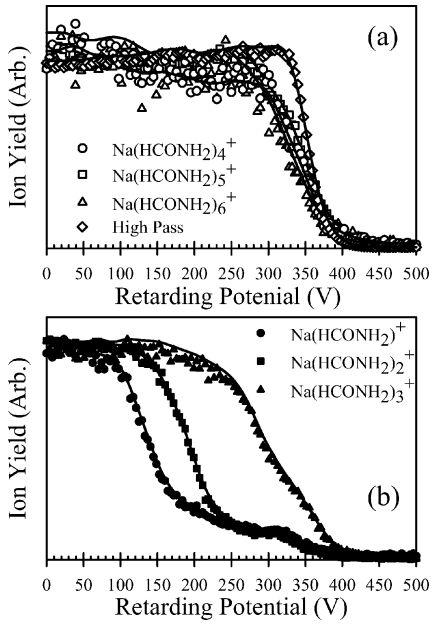

Fig. 8 Retarding voltage curves for the mass-selected $Na^+(HCONH_2)_n$ ions: a) $n = 4$–6 and b) $n = 1$–3. For the "high-pass" measurement, that mass filter was set to transmit ions with mass higher than the $n = 8$ solvated ion (383 amu). Symbols represent the data points while the solid lines represent corresponding smoothed data.

550 V. "High Pass" in Fig. 8a corresponds to an rf-only setting of the quadrupole mass filter that transmits all charged particles above a mass corresponding to an $n = 8$ solvated ion with the possible inclusion of droplets. The m/q of the droplets exceeds the range of the mass filter. The high-pass retarding curve shows a relatively sharp cutoff at a retarding grid potential of 350 V. This signifies a 200-V drop in the charged-particle formation potential in comparison with the capillary potential. Interestingly, the voltage drop, also observed in the TOF instrument, does not depend strongly on the extraction voltage and is found to be more a function of the thruster output current.

The other retarding curves shown in Fig. 8 were recorded by setting the mass filter to the m/q of a particular solvated ion

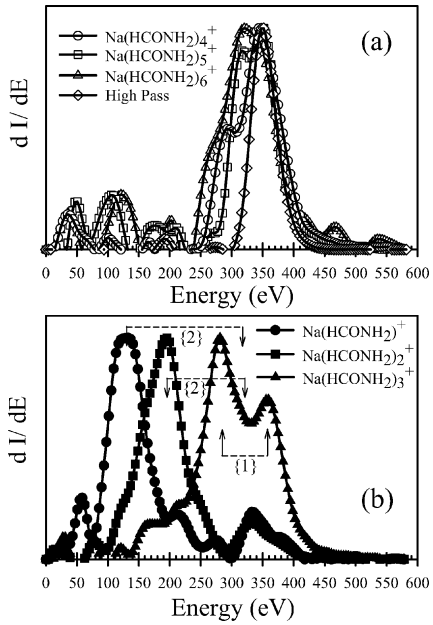

Fig. 9 Energy distribution of the mass-selected $Na(HCONH_2)_n^+$ ions where a) $n = 1$–3 and b) $n = 4$–6. A pair of arrows, connecting by a dotted line, is used to indicate the lost of solvent molecules from the energies of the $Na(HCONH_2)_n^+$ ions ($n = 1$–3), assuming that the solvent evaporation occurs in the field-free region of the apparatus. The corresponding number of solvent lost is indicated in the braces.

and scanning the retarding grid voltage. The heavier solvated ions $n = 4$–6 also shown in Fig. 8a behave similarly to the high-pass measurement but have a slightly broader current drop centered at ~320 V. The curves for solvated ions ($n = 1$–3) are shown in Fig. 8b. These ions exhibit substantially broader current cutoff regions that have structure and extend to lower voltages. Figures 9a and 9b show the derivates of the retarding curves in Fig. 8. The derivatives correspond to the energy distributions of the respective ions. In Fig. 9a, the energy distributions of the high-pass particles have a width of 50 eV full width at half maximum (FWHM) centered at 350 V, whereas the ions ($n = 4$–6), have a broader distribution with a width of ~100 eV (FWHM) centered at ~320 eV.

The energy distributions of the smallest solvated ions shown in Fig. 9b clearly exhibit multiple peaks. Each of the three distributions has a high-energy peak that is centered at 330–350 V, similar to the heavier ions. A second more intense peak at lower voltages is also observed for each of the distributions. Structured energy distributions have also been seen in electrohydrodynamic ionization studies by Huberman[12] and Simons et al.[13] Those glycerol solution studies were conducted at significantly higher extraction voltages in a high-current, multicone regime of operation. The multiple peaks were attributed to metastable decay of solvated ions in the field-free regions of their experiment. The loss of solvent molecules in a field-free region prior to the mass analyzer will result in an ion energy E:

$$E = [(m_0 - l \times m_s)/m_0]E_0 \qquad (2)$$

The arrows and associated numbers in braces in Fig. 9 indicate energy losses corresponding to the respective loss of solvent molecules. It is seen that the positions of the most intense peaks of the $n = 1$–3 ions agree nicely with the predictions for the loss of two, two, and one solvent molecules from larger metastable ions, respectively. Analysis of the $n = 1$–3 energy distributions reveals that 83% of $n = 1$ ions arise from the decay of an $n = 3$ ion, 86% of $n = 2$ ions arise from the decay of an $n = 4$ ion, and 58% of $n = 3$ ions arise from the decay of an $n = 4$ ion, as well. Correction of the mass distribution with respect to the nascent distributions results in a narrower distribution centered at $n = 4$ and raises the average m/q from 193 to 213 amu, thus approaching the TOF value. The TOF experiment does not register metastable decay in the field-free flight region. Closer examination of the energy distributions of the heavier ions suggests that the broadened distributions in comparison to the high-pass distribution may also be attributable to decay from ions with larger solvation numbers. In this case, the change in energy from the loss of a single formamide molecule can no longer be cleanly resolved.

[EMIM][BF_4]

Figure 10 shows a TOF measurement recorded of the ionic liquid, [EMIM][BF_4], operated at the minimal attainable flow rate. Unfortunately, the flow rate is not accurately measured using the bubble method due to the slow bubble formation rate resulting from the high viscosity of the [EMIM][BF_4] propellant (~43 cp) as compared to the NaI/formamide solution (~3.8 cp). The flight distance was 0.78 m and the capillary potential was +1500 V with an extraction voltage of 1500 V. Figure 10 also shows the derivatives of the recorded TOF spectrum. The latter shows two discrete peaks at flight times of 15.6 and 25.6 μs and no peaks occur at long flight times attributable to droplets. Conversion of the TOF peaks, assuming that the ion energies are close to the capillary potential, yields the respective q/m values of $(8.33 \pm 0.38) \times 10^5$ and $(3.09 \pm 0.09) \times 10^5$ C/kg, corresponding to singly charged ions with masses of 115 ± 5 and 311 ± 9 amu. This suggests that positive ions $EMIM^+$ (111 amu) and $[EMIM^+]_2[BF_4^-]$ (309 amu) are observed. The width of the peaks is related to the energy distribution, which is approximately 120 eV (FWHM).

Figure 10 also shows a TOF curve and its derivative obtained when applying −1500 V to the capillary. Again, two steps with no

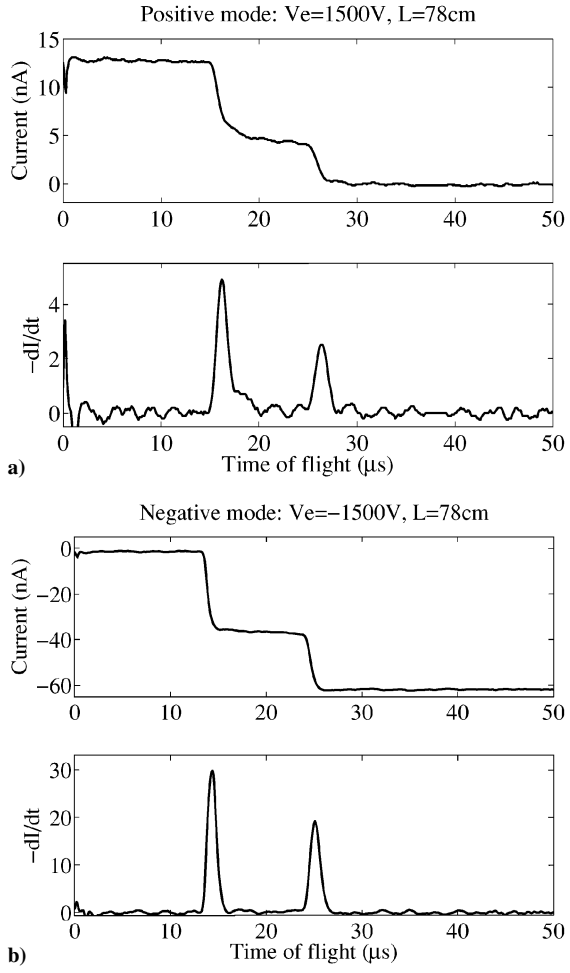

Fig. 10 TOF measurements of [EMIM][BF_4] propellant at minimum flow rate (ion-only emission) and positive and negative bias operation. The capillary potential was ±1500 V. The derivatives are also displayed, exhibiting clear peaks attributable to discrete masses identified with $X^{\pm}$, and $X^{\pm}$[EMIM][BF_4] ions, where X is EMIM or BF_4 for positive and negative bias, respectively.

evidence for droplet formation are observed. The first step occurs at 13.9 μs, whereas the second is located at 24.4 μs. These times convert to specific charges of (10.05 $\pm$ 0.54) and (3.42 $\pm$ 0.09) $\times 10^5$ C/kg, respectively, corresponding to singly charged anions of masses 91.8 $\pm$ 4 and 282 $\pm$ 8 amu. The determined masses again assume that the beam has the same potential as the applied voltage. These masses suggest that the anions BF_4^- (86.8 amu) and $[EMIM^+][BF_4^-]_2$(284.6 amu) are emitted.

[EMIM][BF_4] experiments were conducted at the same minimum-flow-rate conditions in the mass spectrometer. The deposition rate on the QCM was found to be at or below the detection limit. This is consistent with the TOF experiment where exclusively ions were observed. The q/m determined with the near-field Faraday cup thus exceeds 250,000 C/kg. Figure 11 compares typical mass spectra recorded from [EMIM][BF_4] for positive and negative polarities. The predominant ions produced in the positive mode are $[EMIM^+]_n[BF_4^-]_{n-1}$ ($n = 1, 2, 3$), thus confirming the conclusions of the present TOF experiment. The same ion masses have been identified by Romero-Sanz et al.[10,14] In analogy to the positive ion mass spectrum, the negatively biased thruster produces negative ions $[EMIM^+]_{n-1}[BF_4^-]_n$ ($n = 1, 2, 3$) with intensities consistent with the negative-ion TOF measurement in Fig. 10.

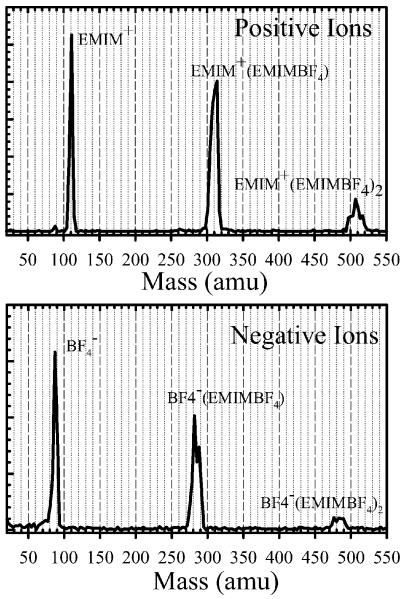

Fig. 11 Mass spectra of [EMIM][BF_4] at minimum flow rate and positive and negative bias operation; extraction voltage was 2700 V. $X^{\pm}$ $([EMIM][BF_4])_n$ ions are identified for $n = 0$–2, where X is EMIM or BF_4 for positive and negative bias, respectively.

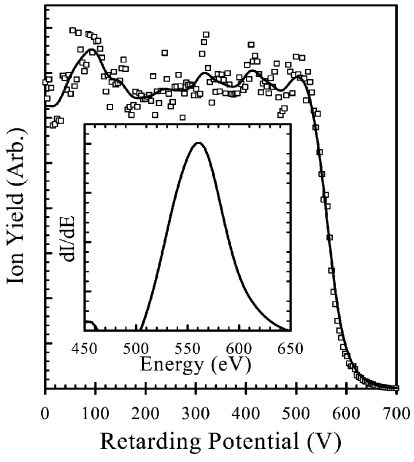

Fig. 12 Retarding potential curve for the $EMIM^+$ ions produced at the conditions of Fig. 11; capillary potential was 550 V. The insert is the corresponding energy distribution.

Figure 12 shows the retarding potential energy curve of the $EMIM^+$ ions as measured with the mass spectrometric experiment in a positively biased operation of [EMIM][BF_4]. The insert is the corresponding energy distribution (derivative) that is centered at ~550 eV, which is also the nominal capillary potential. The energy width of the $EMIM^+$ ions is ~50 eV. A similar energy distribution is also observed for the $[EMIM^+]_2[BF_4^-]$ ions. No evidence of structure attributable to metastables is observed. The analysis of sprayed [EMIM][BF_4] thus reveals that ohmic dissipation losses are negligible in comparison to those observed for the electrolyte solution.

Discussion

The present analysis of colloid thruster plumes from two propellants, an electrolyte solution of NaI dissolved in formamide and the ionic liquid [EMIM][BF_4], has provided new insight with respect to the physics and applicability of colloid thrusters operated in a low-voltage, low-volume-flow-rate single cone-jet mode. Distinctly different behavior is observed for the two propellants at minimum attainable volume flow rates. The output current of the electrolyte solution is predominantly attributable to ions: however, the charged-particle mass flow, and thus the thrust, is governed by a significant droplet fraction. The estimated thrust T and specific impulse I_{sp}, neglecting propellant divergence and assuming 100% propellant utilization efficiency, can be obtained from

$$T = I\,(m/q)\sqrt{2V_a(q/m)} \tag{3}$$

$$I_{sp} = (1/g)\sqrt{2V_a(q/m)} \tag{4}$$

Thrust and specific impulse determined using Eqs. (3) and (4), along with the experimental parameters for the various measurements, are listed in Table 1. Efficiency reductions may occur from emission of neutral or weakly charged droplets. Propellant divergence and propellant utilization efficiency effects have so far been found to be negligible for other propellants operated in a mixed ion/droplet regime (V. Hruby, private communication). The parameters associated with Eqs. (3) and (4) and derived from the NaI/formamide system using both the TOF and mass spectrometer systems are listed in Table 1. Note that, in the table, V_a refers to acceleration voltage as determined by ion energy distribution. The energies of the electrolyte solution ions and droplets suggest that ohmic dissipation losses occur between the capillary and the point in the jet where they are formed. Between ~40 and 110 μW of power are lost to heating of the liquid, corresponding to ~10% of the total electrical power, $(V_c - V_e) \times I$, applied to the system. The table also includes the efficiency defined by the ratio of the power represented by the

Table 1 Representative parameters of operation achieved for the 28.4 wt% NaI/formamide and [EMIM][BF_4] propellants[a]

Propellant	Instr.	I, nA	Q, 10^{-14} m^3/s	q/m, C/kg	V_a, V	T, nN	I_{sp}, s	η, %
NaI/formamide	TOF	600	5	70,000	1,200	111	1,320	49
NaI/formamide	MS	239	2	11,000	1,800	140	640	——
NaI/formamide	MS	227	20	1,500	1,900	360	240	——
[EMIM][BF_4]	TOF	500	——	534,500	1,500	36	3,958	94
[EMIM][BF_4]	TOF	−500	——	−570,200	−1,500	35	4,051	92
[EMIM][BF_4]	MS	500	——	434,090	2,700	50	4,900	92

[a] I and Q represent the total values. The extraction voltage is based on the retarding/stopping potential analysis and thus accounts for the ohmic losses observed for the NaI/formamide case.

thrust and respective mass flow and the applied electrical power:

$$\eta = \frac{T^2/2\dot{m}}{(V_c - V_e)I} = \frac{T^2}{2I^2(V_c - V_e)}\frac{q}{m} \tag{5}$$

Note that thrust T and q/m in Eq. (5) are the average values from the fractional droplet and ion components for the electrolyte solution. No values could be provided for the mass spectrometric instrument because that instrument does not quantify droplet and ion fractions.

The mass spectrum of the electrolyte system exhibits a series of sodium ions solvated by different numbers of formamide molecules. The distribution is peaked at a solvation number of 4. An important fraction of the solvated ions with solvation numbers $n = 1$–3 are observed to be products of metastable decay of larger ions. This decay occurs primarily in the field-free region of the mass spectrometer. This means that the nascent distribution is in fact significantly narrower, consisting primarily of $n = 3$ and 4 ions, and that the thrust is governed not by the m/q distribution observed by the mass spectrometer but by the average value observed by the TOF experiment that is not affected by the metastable decay. It is also possible that the heavier ions observed in the mass spectrometric experiment are also products of decay where we cannot resolve energy distributions associated with loss of a single solvent molecule. Metastability is an indicator of the energy imparted to the solvated ions as they leave the liquid/vacuum interface. To assess the required level of internal excitation to lead to metastability in the gas phase, we have conducted density functional theory calculations of the observed solvated ion structures to estimate the dissociation energies associated with loss of one or two formamide ions. Calculations were conducted at the B3LYP/6-31G(d) level using the Gaussian 98 quantum chemistry package.[15] Geometries were optimized, and normal-mode frequencies for zero-point energy determinations were calculated for formamide and the $n = 1$–6 solvated ions. Table 2 lists the dissociation energies associated with loss of one and two formamide molecules determined for these solvated ions. Mass spectral (Fig. 6) abundances, both recorded and corrected for metastable decay (nascent), are also listed.

Table 2 shows a continuous reduction in bond dissociation energy with increasing solvation number. It is seen that the $n = 4$ solvated ion requires 0.76 and 1.80 eV of internal energy to lose one and two solvent molecules, respectively. From a propulsion point of view, this amount of energy is not significant in comparison to the translational energy imparted to the ion in the field-evaporation process. From the bond dissociation energies calculated at this level, it is not fully apparent why the $n = 4$ solvated ion is the preferred ion in the colloid thruster plume. The derived geometries indicate a closing of a solvation shell at $n = 5$. It may be significant that, in a 28.4% solution, there are 4.6 formamide molecules for every sodium ion. If the limited number of solvent molecules in the vicinity of a sodium ion is the cause of the distribution center at $n = 4$, ions emitted from a more dilute solution may have on average larger solvation numbers.

The solvation number is also limited by the thermal energy that can be accommodated by the ions. This energy grows with the number of internal modes of the molecules that can take up energy. Table 2 also lists calculated molecular room-temperature thermal energies, $E_{\text{th}}(298\ \text{K})$. This is the thermal energy that consists primarily of the excitation of low-frequency vibrational modes and that lies above the molecular zero-point vibrational energy (i.e., $E_{\text{th}}(0\ \text{K}) = 0$). It is seen that the thermal energy exceeds the calculated dissociation energy for $n > 4$. Consequently, according to the calculations at the specified level, a large fraction of $Na^+(HCONH_2)_5$ ions has sufficient energy at room temperature to lose a solvent molecule in the gas phase. The quantum chemical analysis is, therefore, consistent with the observation of reduced intensities for $n > 4$ ions assuming that the ion evaporation occurs from a liquid surface at room temperature.

Table 2 Density functional theory [B3LYP/6-31G(d)] calculations of solvated sodium ion $[Na^+(HCONH_2)_n]$ dissociation energies for one and two solvent molecule loss[a]

n	1	2	$E_{\text{th}}(298)$	I_{raw}	I_{cor}
1	1.73	——	0.15	0.065	0.011
2	1.44	3.16	0.29	0.104	0.015
3	1.04	2.48	0.44	0.187	0.132
4	0.76	1.80	0.59	0.402	0.601
5	0.66	1.42	0.70	0.171	0.171
6	0.31	0.98	0.87	0.038	0.038

[a] $E_{\text{th}}(298)$ is the molecular thermal room-temperature energy above the zero-point energy. All energies are given in electron volts (eV). I_{raw} are the recorded normalized mass spectral intensities (Fig. 6) and I_{cor} are the corrected intensities with respect to the observed decay patterns in Fig. 9.

It is worth noting that this does not preclude observing thermally unstable molecular ions because the lifetime with respect to dissociation increases with the number of vibrational modes for species excited to energies above their dissociation limits.[16,17] In other words, the larger the ion, the longer it can accommodate energy before it is channeled into a dissociation mode, leading to lifetimes that exceed the flight time through the mass spectrometer. The observation of $n > 4$ ions is thus not contradictory to the calculations. Nevertheless, the room-temperature thermal internal energies of the larger solvated ions are significantly above the thresholds for loss of one, and possibly multiple, solvent molecules such that dissociation may be rapid. Thus, solvent molecule loss in the early acceleration stages of the ion flight may be important, which could also be a source of the broadened energy distributions in comparison with the high-pass peak.

Provided the level of theory is sufficiently accurate, the high intensity of $n = 4$ ions suggests that these ions are produced at near room temperature. The dissipative heating discussed earlier may, therefore, not be located in the high-electric-field regions where the ions are evaporated. This is consistent with preliminary model calculations of the cone-jet region by Carretero and Martinez-Sánchez,[18] which demonstrate that maximum ohmic dissipation is slightly displaced from maximum normal electric field along the cone-jet axis.

The ionic liquid, $[EMIM][BF_4]$, was operated in a pure ion-emission mode for both positively and negatively biased operation, as determined from the very high specific charge as well as the plume charged-particle TOF measurements. This signifies a highly efficient, high-specific-impulse mode of operation. TOF and mass spectra resolve individual $X^{\pm}([EMIM][BF_4])_n$ ions, where X is either EMIM or BF_4, respectively. The mass spectrometer detected species $n = 0$–2 for both polarities. Because of the similar performance for both polarities, as concluded from the similar mass spectra, this propellant can be optimally used in an array of an even number of emitters where one half is positively biased and the other half is negatively biased. This would result in a high-specific-impulse engine that does not require a neutralizer. The parameters and derived thrust, specific impulse, and efficiency of the present measurements are also listed in Table 1. Given the high specific charge, the narrow mass distribution, and the lack of measurable ohmic dissipation, the specific impulse and efficiency are very high. Previously, only sulfuric acid has produced a comparable specific impulse in a colloid thruster arrangement.[1]

Quantum chemical calculations for these systems are far more complex and require a molecular dynamics approach to determine the minimum energy geometry. A molecular dynamics investigation (A. T. Yeates, private communication) of the observed $[EMIM][BF_4]$ ions indicates that species $X^{\pm}([EMIM][BF_4])_n$ ($n > 1$) are thermally unstable at room temperature. This is again consistent with the observed mass spectrometric distributions.

Contrary to the electrolyte solution, the charged particles field-evaporated from $[EMIM][BF_4]$ have energies that imply that they are formed at or near the capillary potential. Thus, there are negligible ohmic dissipation losses in the Taylor cone or jet. This is similar to observations in FEEP systems, where very precise energy-deficit measurements have detected losses of less than 10 V that were attributed to the work required to extract an ion from the liquid metal surface.[3] Romero-Sanz et al. did not record SP measurements for this system and assumed an 80–90% reduction in the ion energy with respect to the capillary potential, as was observed for the present electrolyte solution.[10] The lack of ohmic losses may appear puzzling considering that the room-temperature conductivity of the ionic liquid (1.3 S/m) is lower than that of the electrolyte solution

(2 S/m). From the energy distribution of the ions, it is seen that a significant fraction of ions exceeds the capillary potential. One possible explanation could be significant space charge at the point of ion emission; however, this should result in a substantial attenuation of the emitted ion beam, which we do not observe when compared with the electrolyte solution. We currently do not have an explanation for this observation.

No metastability is observed in the energy distributions of the mass spectrally resolved ions from [EMIM][BF4]. If thermal stability is the determining factor for the ion masses observed in the colloid thruster plumes, this suggests that thermally unstable ionic liquid ions decay more rapidly than the electrolyte ions. The decay would, therefore, occur close to the jet in the acceleration region and, thus, would not result in structure in the observed energy distributions.

Conclusions

Complementary TOF and quadrupole mass spectrometric methods are applied to studying colloid thrusters operated with two different propellants: 28.4 wt% NaI in formamide and [EMIM][BF_4]. Whereas the TOF approach collects the entire thruster plume, the quadrupole experiment provides detailed measurements of mass and energy distributions of field-evaporated ions accelerated into a small solid angle. The NaI/formamide solution is found to produce a distribution of solvated ions, $Na^+(HCONH_2)_n$, centered at $n = 4$. Ions with $n < 4$ are predominantly the result of solvent molecule loss from larger ions during the flight through the mass spectrometer, as determined from the structured mass-resolved energy distributions. The predominance of $n = 4$ ions may have its roots in the stochiometric availability of formamide molecules (4.6 per sodium ion) in the 28.4 wt% solution. However, density functional calculations of the bond dissociation and thermal energies of the ions suggest that ions with $n > 4$ are unstable at room temperature. Droplets and ions observed for the electrolyte solution are formed at a potential that is lower than the capillary potential by approximately 200 V, implying dissipative ohmic losses in the Taylor cone.

In the case of the ionic liquid, [EMIM][BF_4], pure ion emission is observed at low flow rates in both positive and negatively biased operation, resulting in a thruster with a specific impulse of about 4000 s without additional ion acceleration. The high efficiency of the [EMIM][BF_4] colloid thruster is further evidenced by the lack of ohmic losses as manifested by the ion energy distributions.

Acknowledgments

This work was supported by the Air Force Office of Scientific Research (AFOSR) (program managers Mitat Birkan and Michael Berman) as part of the AFOSR Space Miniaturization Theme. The authors are grateful to Juan Fernandez de la Mora, David Luedtke, and Uzi Landman for helpful comments. The authors thank A. Todd Yeates for communicating his theoretical results prior to publication.

References

[1]Perel, J., Mahoney, J. F., Moore, R. D., and Yahiku, A. Y., "Research on a Charged Particle Bipolar Thruster," AIAA Paper 67-728, Sept. 1967.

[2]Huberman, M. N., and Rosen, S. G., "Advanced High-Thrust Colloid Sources," *Journal of Spacecraft*, Vol. 11, No. 7, 1974, pp. 475–480.

[3]Prewett, P. D., and Mair, G. L. R., *Focused Ion Beams from Liquid Metal Ion Sources*, Wiley, New York, 1991.

[4]Gamero-Castaño, M., and Fernández de la Mora, J., "Direct Measurement of Ion Evaporation Kinetics from Electrified Liquid Surfaces," *Journal of Chemical Physics*, Vol. 113, No. 2, 2000, pp. 815–832.

[5]Gamero-Castaño, M., and Hruby, V., "Electrospray as a Source of Nanoparticles for Efficient Colloid Thrusters," AIAA Paper 2000-3265, July 2000.

[6]Gamero-Castaño, M., and Hruby, V., "Electrospray as a Source of Nanoparticles for Efficient Colloid Thrusters," *Journal of Propulsion and Power*, Vol. 17, No. 5, 2001, pp. 977–987.

[7]Loscertales, I. G., and Fernandez de la Mora, J., "Experiments on the Kinetics of Field Evaporation of Small Ions from Droplets," *Journal of Chemical Physics*, Vol. 103, No. 12, 1995, pp. 5041–5060.

[8]Lozano, P., and Martinez-Sánchez, M., "Experimental Measurements of Colloid Thruster Plume in the Ion-Droplet Mix Region," AIAA Paper 2002-3814, July 2002.

[9]Lozano, P., "Studies on the Ion-Droplet Mixed Regime in Colloid Thruster," Ph.D. Dissertation, Dept. of Aeronautics and Astronautics, Massachusetts Inst. of Technology, Cambridge, MA, 2003.

[10]Romero-Sanz, I., Bocanegra, R., Fernandez de la Mora, J., and Gamero-Castano, M., "Source of Heavy Molecular Ions Based on Taylor Cones of Ionic Liquids Operating in the Pure Ion Evaporation Regime," *Journal of Applied Physics*, Vol. 94, No. 5, 2003, pp. 3599–3605.

[11]Chiu, Y., Levandier, D. J., Austin, B. L., Dressler, R. A., Murray, P. T., Lozano, P., and Martinez-Sanchez, M., "Mass Spectrometric Analysis of Ion-Emission from Selected Colloid Thruster Fuels," AIAA Paper 2003-4848, July 2003.

[12]Huberman, M. N., "Measurement of the Energy Dissipated in the Electrostatic Spraying Process," *Journal of Applied Physics*, Vol. 41, No. 2, 1970, pp. 578–584.

[13]Simons, D. S., Colby, B. N., and Evans, J. C. A., "Electrohydrodynamic Ionization Mass Spectrometry—The Ionization of Liquid Glycerol and Non-Volatile Organic Solutes," *International Journal of Mass Spectrometry and Ion Physics*, Vol. 15, No. 3, 1974, pp. 291–302.

[14]Romero-Sanz, I., and Fernandez de la Mora, J., "Spatial Structure and Energy Distribution of Electrosprays of Ionic Liquids in Vacuo," *Journal of Applied Physics*, Vol. 95, No. 4, 2004, pp. 2123–2129.

[15]Frisch, M. J., Trucks, G. W., Schlegel, H. B., Scuseria, G. E., Robb, M. A., Cheeseman, J. R., Zakrzewski, V. G., Montgomery, J. A., Stratmann, R. E., Burant, J. C., Dapprich, S., Millam, J. M., Daniels, A. D., Kudin, K. N., Strain, M. C., Farkas, O., Tomasi, J., Barone, V., Cossi, M., Cammi, R., Mennucci, B., Pomelli, C., Adamo, C., Clifford, S., Ochterski, J., Petersson, G. A., Ayala, P. Y., Cui, Q., Morokuma, K., Malick, D. K., Rabuck, A. D., Raghavachari, K., Foresman, J. B., Cioslowski, J., Ortiz, J. V., Stefanov, B. B., Liu, G., Liashenko, A., Piskorz, P., Komaromi, I., Gomperts, R., Martin, R. L., Fox, D. J., Keith, T., Al-Laham, M. A., Peng, C. Y., Nanayakkara, A., Gonzalez, C., Challacombe, M., Gill, P. M. W., Johnson, B., Chen, W., Wong, M. W., Andres, J. L., Gonzalez, C., Head-Gordon, M., Replogle, E. S., and Pople, J. A., Gaussian 98, Revision A.6 ed., Gaussian, Pittsburgh, PA, 1998.

[16]Holbrook, K. A., Pilling, M. J., and Robertson, S. H., *Unimolecular Reactions*, 2nd ed., Wiley, New York, 1996.

[17]Gilbert, R. G., and Smith, S. C., *Theory of Unimolecular and Recombination Reactions*, Blackwell Scientific, Oxford, UK, 1990.

[18]Carretero, J., "Numerical Studies of a Single Emitter Colloid Thruster in the Pure Droplet and Mixed Regimes," Ph.D. Dissertation, Dept. of Aeronautics and Astronautics, Massachusetts Inst. of Technology, Cambridge, MA, 2004.